NANO LETTERS

2003
Vol. 3, No. 8
1097−1101

Rectifying Behavior of Electrically Aligned ZnO Nanorods

Oliver Harnack,*,† Claudia Pacholski,‡ Horst Weller,‡ Akio Yasuda,† and Jurina M. Wessels†

Materials Science Laboratories, Sony International (Europe) GmbH, Sony Corporate Laboratories Europe (SCLE), Hedelfinger Strasse 61, 70327 Stuttgart, Germany, and Institute of Physical Chemistry, University of Hamburg, Bundesstrasse 45, 20146 Hamburg, Germany

Received April 18, 2003; Revised Manuscript Received June 2, 2003

ABSTRACT

We report on the electrical alignment of ZnO nanorods and their electrical properties. The ZnO nanorods were wet-chemically synthesized, and their length and diameter were adjusted to about 200−300 nm and 15−30 nm, respectively. The nanorods were deposited onto electrode structures and directed into 200- to 800-nm-wide electrode gaps by using alternating electric fields at frequencies between 1 and 10 kHz and field strengths between 10^6 and 10^7 V/m. The nanorods align parallel to the electric field lines and make electrical contact with the gold electrodes. Clear photoresponse to 366-nm ultraviolet light irradiation was demonstrated. The current−voltage characteristics of the aligned rods are strongly nonlinear and asymmetrical, showing rectifying, diode-like behavior and asymmetry factors up to 25 at 3-V bias voltage.

The continuous downscaling of the feature sizes of microelectronic devices well below 100 nm[1] has initiated an enormous amount of research activity on alternatives to traditional electronic components such as complimentary metal oxide semiconductor (CMOS)-based field-effect transistors and lithographically defined interconnects. The demand for alternative device concepts is related to the expectation that downscaling of conventional CMOS devices will reach physical limits within the next few years.[2]

For the patterning technology, optical lithography will still be the method of choice for mass production because of its high throughput capabilities.[3] However, the development of optical lithography tools for continuously decreasing feature sizes will become increasingly expensive. Thus, radical new device and fabrication concepts that offer high performance and low price are required.

A current trend is to invent device concepts based on unique nanostructures of materials such as insulators, semiconductors, metals, or combinations of these materials. Nanorods and tube-shaped nanostructures have been fabricated recently using cheap and simple wet-chemical and physical synthesis methods. Semiconducting tubes and nanorods have been made from CdSe, CdTe, ZnO, and others, and they have shown a large variety of properties such as chemical sensing,[4] luminescence,[5] field effects,[6] lasing,[7] and photoresponse.[8] Synthesis concepts are well established; however, there is less experience to date on the alignment of nanostructures to build working electronic devices or to integrate them into complex architectures.[9] Unconventional lithography approaches such as microcontract printing[10] or dip-pen lithography[11] have the potential to control nanostructure assembly. The funtionalization of carbon nanotubes toward the directed self-assembly and alignment of more complex nanostructures has already been demonstrated.[12] Here, we describe the successful alignment of wet-chemically synthesized, semiconducting ZnO nanorods in the suspension phase using an electric field to place them onto predefined electrodes. We also demonstrate their unique properties such as photoresponse and current rectification.

Synthesis. ZnO nanorods were prepared according to a method described earlier.[13] Briefly, 29.5 g (0.13 mol) of zinc acetate dihydrate was dissolved in 125 mL of methanol at 60 °C. Then, a solution of 14.8 g (0.23 mol) of potassium hydroxide in 65 mL of methanol was added. The reaction mixture was stirred for several days at 60 °C. During this time, the nanoparticles precipitate. The length and the width of the resulting nanorods depend on the reaction time. The length of the nanorods increased considerably with longer reaction times, but the width of the nanorods grew only slightly. The precipitate was washed with methanol and centrifuged (5500 rpm, 30 min), and the resulting gel was redispersed in chloroform. The nanoparticles were diluted with a mixture of ethyleneglycol/water (2:1). Figure 1 shows a TEM image of ZnO nanorods after a reaction time of 3 days. The nanorods have a diameter of 15 to 30 nm and a length of 200 to 300 nm.

* Corresponding author. E-mail: harnack@sony.de. Phone: +49 711 5858 212. Fax: +49 711 5858 484.
† Sony Corporate Laboratories Europe.
‡ University of Hamburg.

10.1021/nl034240z CCC: $25.00
Published on Web 06/24/2003

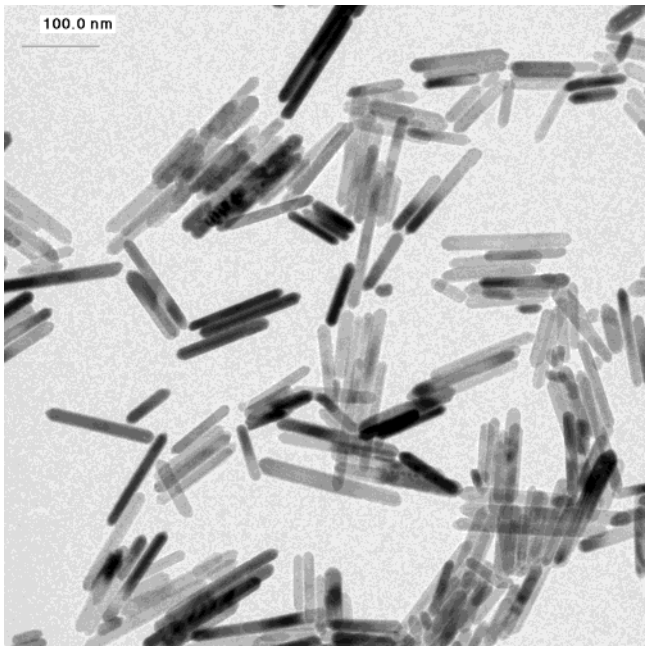

Figure 1. TEM image of ZnO nanorods after a reaction time of 3 days.

Electrical Alignment. The manipulation and alignment based on dielectrophoretic forces in an alternating electric field were demonstrated for a number of different structures such as DNA molecules,[14] gold nanowires,[15] and carbon nanotubes[16] as well as for metal and semiconducting nanoparticles.[17] In all cases, the electric field induces charge separation, and the resulting polarization generates a dipole moment, which aligns the structure to an energetically favorable orientation (i.e., parallel to the field lines). In addition, if the field distribution is nonuniform, then a dielectric force that points into the direction of the highest field density acts on the polarized structure. The dielectrophoretic force, F, is given by the following expression:

$$F = \frac{1}{2}\alpha\nu\nabla|E|^2 \qquad (1)$$

where α is the effective polarizability of the structure, E is the electric field strength, ∇ is the gradient vector operator and, ν is the structure volume. This force is responsible for the movement of the polarized structure toward the electrode edges where the electric field density has the highest value.[18] The alignment force is frequency-dependent because the polarizability of the nanostructure and the surrounding solvent changes with frequency.[19]

We have chosen the frequency range between 1 and 10 kHz where the polarization of the nanorods dominates the polarization of the solvent molecules so that effective electrical alignment of the ZnO nanorods is possible. At much higher frequencies, the aligning force vanishes again. An HP source measure unit[20] was used to generate the electric field at various strengths and frequencies. The sample was mounted on a chip carrier and wire bonded using 25-μm-thick aluminum wires to provide electrical connections. The electrode structures were fabricated on 400-nm-thick silicon oxide using standard electron beam lithography and a lift-off technique. The electrode material was thermally evaporated chrome (5 nm) and gold (50 nm) on top. Typically, after applying one drop of approximately 1 mM concentrated ZnO nanorods in ethylene glycol/water to the electrode structure, the field was switched on. Depending on the gap size, the driving voltage was gradually increased from zero to about 6 V_{pp} to 20 V_{pp} (peak-to-peak) so that the electric field strength was in the range between 10^6 and 10^7 V/m at 1 to 10 kHz. The field was applied for about 20 s; subsequently, the sample was washed using one drop of ethylene glycol. After this, the surface was dried using compressed air, and finally, the field was switched off.

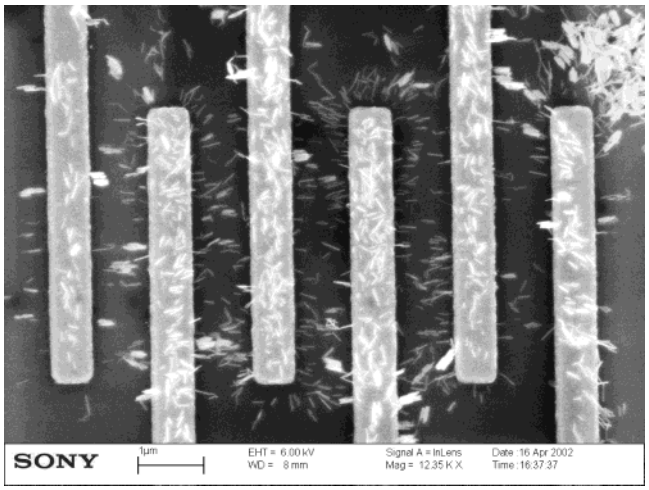

Figure 2. Electrically aligned ZnO nanorods between 800-nm spaced, interdigitated gold electrodes on silicon oxide. The electrode fingers on the bottom and on the top were on the same potential. The applied electric field strength was 1.25×10^7 V/m, and the frequency was 1 kHz.

Figure 2 shows a scanning electron microscopy (SEM) picture of a sample that was treated using the described method. The gap size between the interdigitated finger electrodes was about 800 nm, and the applied voltage was 20 V_{pp} at 1 kHz, corresponding to a field strength of 1.25×10^7 V/m. The nanorods obviously follow the electric field direction by aligning parallel to the flux lines. Nanorods on top of the electrodes are not aligned because the electric field strength and therefore the resulting force is zero at these spots (eq 1).

To contact both ends of the nanorods to electrodes, the alignment experiment was repeated on electrodes with smaller gaps of about 200 nm. Figure 3A shows an SEM picture of an electrode array (sample 1) after one drop of the ZnO nanorod solution at a concentration of approximately 1 mM was applied and the voltage was increased to 5 V_{pp} between electrodes 1 and 2, corresponding to a maximum field strength of 1.25×10^7 V/m at 10 kHz. The operating frequency was increased to 10 kHz because some of the 200-nm-gap electrodes tend to get damaged at 1 kHz. From the SEM picture, it is obvious that most of the nanorods were collected in the gap between electrodes 1 and 2; a few rods

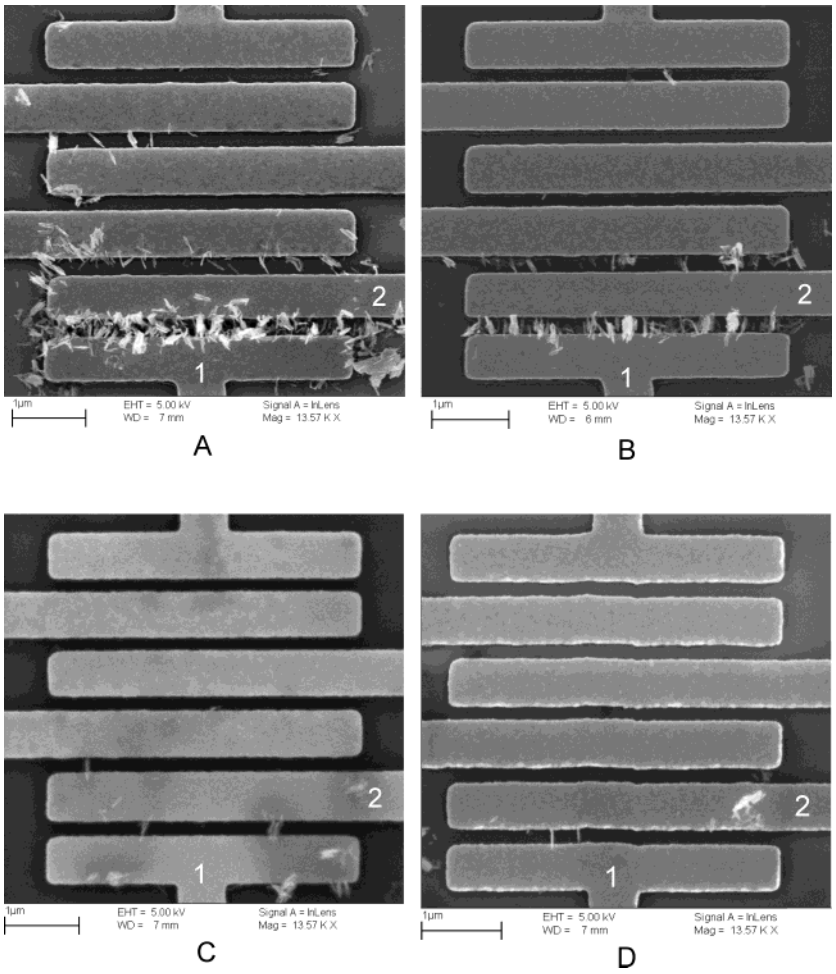

Figure 3. Electrically aligned ZnO nanorods between 200-nm spaced gold electrodes. The applied electric field strength was 1.25×10^7 V/m, and the frequency was 10 kHz. The following concentrations were used: (A) ZnO nanorod stock concentration of approximately 1 mM (sample 1); (B) 50% diluted stock in ethylene glycol/water (sample 2); (C) and (D) 66% diluted stock (samples 3 and 5).

were located in other gaps. However, the alignment is quite disordered because a large fraction of the rods are not aligned parallel to the field direction.

In another experiment, the concentration of the ZnO nanorod suspension was reduced by a factor of 2 while keeping the electrical alignment parameters fixed. The SEM picture in Figure 3B (sample 2) shows fewer nanorods assembled in the gap than for the previous case. In a third (sample 3), fourth (sample 4), and fifth experiment (sample 5), the initial ZnO nanorod concentration was diluted by a factor of 3. These samples show only very few nanorods assembled between the connected electrodes 1 and 2 (Figure 3C/sample 3 and Figure 3D/sample 5). These results clearly demonstrate that the ZnO nanorods can be easily aligned in electric fields, which oscillate at frequencies between 1 and 10 kHz. The number of rods can be controlled by the concentration of the ZnO nanorod suspension.

Electrical Characterization. The aligned ZnO rods were electrically characterized by using an HP source measuring unit[21] in a two-probe configuration and in voltage bias mode. The resistance of the nanorod assemblies, R_{dark}, was high, on the order of about 1−4 GΩ at a bias of 1 V. (The baseline was about 10 GΩ.) As shown in Table 1, there is just a weak scaling of R_{dark} with the number of nanorods. The high resistivity is governed by the wide ZnO band gap of about 3.3 eV, corresponding to a wavelength of about 373 nm.[22] The conductivity can be enhanced by doping, temperature increase, or ultraviolet (UV) light-induced photoconductivity. Table 1 summarizes the resistance, R_{UV}, of the investigated nanorod assemblies under 366-nm UV light irradiation at about 0.1 W/cm^2. The resistance of all samples decreased significantly as the UV light was switched on at a bias voltage of 1 V. The estimated resistance per rod under UV light was about 1 GΩ at a bias of 1 V, which includes also the contact resistance. The change in resistance $\Delta R(U) = R_{dark}(U) - R_{UV}(U)$ increased with increasing bias voltage. Figure 4 shows the time-dependent photoresponse for one to two contacted nanorods (sample 5, Figure 3D). A control

Table 1. Electrical Data of ZnO Nanorod Assembly Samples

sample number	number of nanorods	R_{dark}/MΩ at 1 V	R_{UV}/MΩ at 1 V	IVC asymmetry at 3 V
1	>100	1200	20	1
2	∼50	1000	40	12
3	∼6	3000	300	12
4	∼4	1000	250	13
5	1−2	4000	500	25

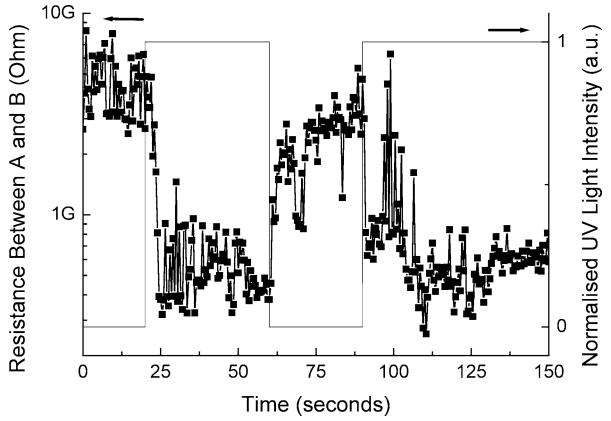

Figure 4. Time-dependent photoresponse of sample 5 (shown in Figure 3D) at a bias voltage of 1 V.

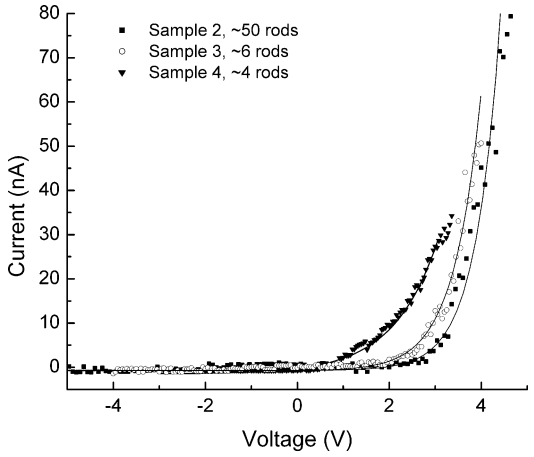

Figure 5. IVCs of ZnO nanorod assemblies with different numbers of nanorods. The solid curves represent fits based on eq 2.

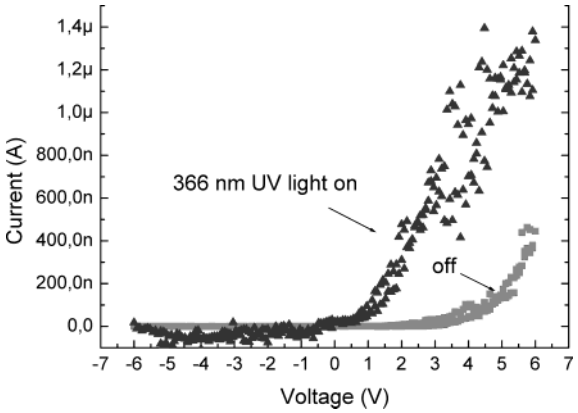

Figure 6. IVC of ZnO nanorod sample 2 with and without 366-nm UV illumination.

experiment on an electrode structure without ZnO nanorods in the gap showed no photoresponse.

The photoresponse of ZnO is due to the photoadsorption and desorption of oxygen.[23] In the dark, oxygen is adsorbed on the surface of ZnO in form of negatively charged ions by capturing free electrons from the n-doped semiconductor, leading to a depletion layer with low electrical conductivity on the surface. UV light absorption generates electron−hole pairs, and the holes oxidize the adsorbed negatively charged oxygen ions at the surface while the remaining electrons in the conduction band increase the conductivity.[24] This may help to explain why, in contrast to the behavior of R_{dark}, R_{UV} more clearly scales with the number of assembled nanorods (Table 1). The large surface resistance in the dark probably leads to large contact resistance between the nanorod and the metal electrode. This dominates the over-all assembly resistance regardless of the number of nanorods between the electrodes. However, under UV irradiation, the depletion layer on the nanorod surface vanishes, and the contact resistance decreases significantly. Thus, under UV light, the over-all assembly resistance shows a more pronounced dependence on the amount of nanorod material in the gap.

Samples 1 and 4 showed a certain anomalous trend for both R_{dark} and R_{UV}. For sample 1, a high nanorod density with a high degree of disorientation is present in the gap. We assume that because of a dominating contact resistance, there is no clear reduction of R_{dark} in comparison to sample 2.[35] However, R_{UV} is two times smaller, presumably because of more conducting material inside the gap. Sample 4 showed a surprisingly low R_{dark}, which may indicate very good electrical contact between the very few rods and the electrodes. This also seems to result in a relatively low R_{UV}.

In addition to the photoresponse, our nanorods showed surprisingly strong nonlinear and asymmetric current−voltage characteristics (IVC). As displayed in Figure 5 for three different samples, the IVCs show current rectification for the aligned ZnO nanorods (i.e., little current flows in reverse bias, whereas there is a sharp current onset in forward bias). The IVC asymmetry factor varied between 10 and 25 at a bias voltage of 3 V, and it increased with the decreasing number of rods between the electrodes. The factors are given in Table 1 for different samples. This kind of diodelike behavior was repeatedly observed for a large number of aligned ZnO nanorod assemblies. Nonaligned assemblies that were fabricated by spin coating generally exhibited symmetrical IVCs. In this case, the direction of the nanorod alignment was statistically distributed without any dominant orientation.

UV light irradiation also has a strong impact on the diode current levels as shown for sample 2 in Figure 6. Analogous to the photoresponse to UV light mentioned earlier, we find up to about a 2 orders of magnitude increase of the diode current in the forward bias direction at 2 V and under 366-nm irradiation. A striking feature is the relatively noisy IVC when the UV irradiation is turned on, possibly because of the trapping and detrapping of photoexcited carriers at the nanorod−electrode interface, leading to telegraph-like noise. This shows that the interface properties between the gold electrode and the ZnO nanorod have a dominant impact on the transport properties.

Asymmetric IVCs were also recently reported for CdSe nanorods and SnO_2 nanowires.[25] The origin of the asymmetric behavior, however, is not clear yet, and we also can only speculate on the basis of our new experimental data. Differences in the barrier properties on both sides of the metal−semiconductor−metal Schottky junctions are probably responsible for the observed electrical behavior.[26]

The diode current, I, across a Schottky barrier is given by the general expression[27]

$$I = I_S\left\{\exp\left(\frac{e(V - V_{th})}{nk_BT}\right) - 1\right\} \quad (2)$$

where V_{th} is the threshold voltage, n is the ideality factor, k_B is the Boltzmann factor, T is the operating temperature, and I_S is the saturation current. Fits of the experimental data from different samples using eq 2 yield n between 20.5 and 38 (Figure 5). Such a large deviation from the ideal case (n = 1, thermionic emission model[27]) was reported earlier for Schottky barriers based on metal/semiconducting polymer junctions[28] and also recently for Schottky diodes made from GaN nanowires.[29] A large n was attributed to an insulating interfacial layer between the metal electrode and the semiconductor surface.[30]

An electrical asymmetry could be induced by a dipole moment in nanocrystals with wurtzite structure.[31−34] In ZnO, zinc and oxygen layers alternate along the c axis so that a resulting dipole moment could lead to a potential gradient that influences the symmetry of current flow. However, because the dipole orientation should vary statistically between the rods, another explanation could be that different barrier heights are formed during the deposition process itself (e.g., the rods might be fixed better to one of the electrodes due to field inhomogenities) or may result from irreversible Faraday processes that occur under initial polarization when measuring the IVCs. Further experiments are required to identify the origin of the rectifying behavior of the nanorods.

Conclusions. We have shown that ZnO nanorods can be directed and aligned effectively by using alternating electric fields. The resulting assemblies show a strong photoresponse and nonlinear, rectifying current−voltage characteristics. The origin of the strong asymmetry is possibly due to asymmetric interfacial barrier properties (e.g., different Schottky barrier heights on both ends of the aligned nanorod). Such nanostructures are potentially useful for realizing rectifying nanodiodes, optical nanoswitches, and nanointerconnects.

Acknowledgment. This work was partially funded by the European Commission through the IST-FET Nanotechnology Information Devices initiative, BIOAND project IST-1999-11974.

References

(1) *International Technology Roadmap for Semiconductors* (ITRS), http://public.itrs.net/.
(2) Hutchby, A.; Bourianoff, G. I.; Zhirnov, V. V.; Brewer, J. E. *IEEE Circuits & Devices Magazine* **2002**, *March*, 28−41.
(3) Harriott, L. R. *Proc. IEEE* **2001**, *89*, 366.
(4) Cui, Y.; Wei, Q.; Park, H.; Lieber, C. M. *Science 293*, 1289−1292.
(5) Huang, M. H.; Wu, Yiying; Feick, H.; Tran, N.; Weber, E.; Yang, P. *Adv. Mater.* **2001**, *13*, 113−116.
(6) Duan, X.; Huang, Y.; Lieber, C. M. *Nano Lett.* **2002**, *2*, 487−490.
(7) Johnson, J. C.; Yan, H.; Schaller, R. D.; Haber, L. H.; Saykally, R. J.; Yang, P. *J. Phys. Chem. B* **2001**, *105*, 11387−11390.
(8) Kind, H.; Yan, H.; Messer B.; Law, M.; Yang, P. *Adv. Mater.* **2002**, *14*, 158−160.
(9) Service, R. F. *Science* **1999**, *286*, 2442−2444.
(10) Xia, Y.; Whitesides, G. M. *Angew. Chem.* **1998**, *110*, 568.
(11) Piner, R. D.; Zuh, J.; Xu, F.; Hong, S.; Mirkin, C. A. *Science 283*, 661.
(12) Williams, K. A.; Veenhuizen, P. T. M.; Torre, B. G. de la; Eritja, R.; Dekker, C. *Nature 420*, 761.
(13) Pacholski, C.; Kornowski, A.; Weller, H. *Angew. Chem., Int. Ed.* **2002**, *41*, 1188−1191.
(14) Susuki, S.; Yamanashi, T.; Tazawa, S.; Kurosawa, O.; Washizu, M. *IEEE Trans. Ind. Appl.* **1998**, *34*, 75−83.
(15) Smith, P. A.; Nordquist, C. D.; Jackson, T. N.; Mayer, T. S.; Martin, B. R.; Mbindyo, J.; Mallouk, T. E. *Appl. Phys. Lett.* **2002**, *77*, 1399−1401.
(16) Krupke, R.; Hennrich, F.; Weber, H. B.; Hampe; Kappes, M. M.; v. Löhneysen, H. Unpublished work, 2002.
(17) Bezryadin, A.; Dekker, C. *Appl. Phys. Lett.* **1997**, *71*, 1273−1275.
(18) Pohl, H. A. *J. Appl. Phys.* **1915**, *22*, 869−871.
(19) Bockris, J. O'M.; Reddy, A. K. N. *Modern Electrochemistry: An Introduction to an Interdisciplinary Area*; Plenum Press: New York, 1970.
(20) Model DSR 345, Standford Research.
(21) Model HP4142, Hewlett Packard.
(22) Srikant, V.; Clarke, D. R. *J. Appl. Phys.* **1998**, *83*, 5447−5451.
(23) Zhang, D. H. *J. Phys. D* **1995**, *28*, 1273−1277.
(24) For this reason, the photoresponse is slow in vacuum or in an inert gas atmosphere and fast if oxygen is available. The measurements we report here were all made under ambient atmospheric conditions.
(25) Law, M.; Kind, H.; Messer, B.; Kim, F.; Yang, P. *Angew. Chem.* **2002**, *114*, 2511−2514.
(26) At both metal−semiconductor interfaces, electrons leave from the semiconductor into the metal, building up an inner potential, which represents a barrier for further current flow once equilibrium between electron diffusion into the metal and the drift of electrons due to the inner field has been reached.
(27) Milnes, A. G.; Feucht, D. L. *Heterojunctions and Metal−Semiconductor Junctions*; Academic Press: New York, 1972.
(28) Gupta, R.; Misra, S. C. K.; Malhotra, B. D.; Beladakere, N. N.; Chandra, S. *Appl. Phys. Lett.* **1991**, *58*, 51.
(29) Kim, J.-R.; Oh, H.; So, H. M.; Kim, J.-J.; Kim, J.; Lee, C. J.; Lyu, S. C. *Nanotechnology* **2002**, *13*, 701−704.
(30) Tyagi, M. S. In *Metal−Semiconductor Schottky Barrier Junctions and Their Applications*; Sharma, B. L., Ed.; Plenum Press: New York, 1984.
(31) Colvin, V. L.; Alivisatos, A. P. *J. Chem. Phys.* **1992**, *97*, 730−733.
(32) Empedocles, S. A.; Bawendi, M. G. *Science* **1997**, *278*, 2114−2117.
(33) Blanton, S. A.; Leheny, R. L.; Hines, M. A.; Guyot-Sionnest, P. *Phys. Rev. Lett.* **1997**, *79*, 865−868.
(34) Shim, M.; Guyot-Sionnest, P. *J. Chem. Phys.* **1999**, *111*, 6955−6964.
(35) It is also possible that because of the high disorientation in sample 1 the number of working ZnO nanorod−electrode junctions may not be much higher than for the case of sample 2.

NL034240Z